scientific reports

Check for updates

OPEN

Exploring the anti-inflammatory activity of fupenzic acid using network pharmacology and experimental validation

Djoudi Boukerouis[1,2,3,4,6], Irene Cuadrado[3,6], Nadjet Debbache Benaida[1], Ana Estévez-Braun[2], Beatriz de las Heras[3]✉, Angel Amesty[2]✉ & Sonsoles Hortelano[5]✉

Crataegus azarolus **L. (Rosaceae), commonly known as Mediterranean hawthorn, has long been valued in Traditional Medicine for treating cardiovascular and inflammation-related diseases, including diabetes, cancer, and rheumatism. Pharmacological benefits of *Crataegus azarolus* L. are notably linked to its anti-inflammatory properties. Fupenzic acid, a pentacyclic triterpene isolated from its leaves, holds significant pharmacological potential that remains elusive. This study investigates the unexplored capacity of fupenzic acid as a promising anti-inflammatory agent. Using a multidisciplinary approach that integrates network pharmacology, molecular docking, in vitro assays, and predictive in silico analyses of drug-like properties, ADME, and toxicity, the mechanisms and properties of fupenzic acid have been elucidated. Network pharmacology analysis identified the potential targets for fupenzic acid, with enrichment analyses revealing key processes like inflammatory response, cytokine signaling, innate immune system, and MAPK cascade regulation. Transcription factors such as RELA, SP1, and NFKB1 were predicted to play crucial roles in its therapeutic effects. PPI network analysis underscored NF-κB as a central hub, linking these pathways to its anti-inflammatory effects. In vitro experiments demonstrated that fupenzic acid effectively suppressed inflammatory mediators like NOS-2 and COX-2, through the NF-κB pathway. Molecular docking further confirmed its favorable interaction with NF-κB, reinforcing its mechanism of action. Additionally, in silico ADMET profiling revealed favorable drug-like properties including pharmacokinetics and toxicity profiles, emphasizing its suitability as a drug candidate. This study represents a major step forward in understanding the therapeutic potential of fupenzic acid, establishing it as a distinctive and promising anti-inflammatory agent. The findings identified it as a pharmacological agent for clinical development targeting inflammation-driven diseases and also provide a foundation for future translational research.**

Keywords Fupenzic acid, Triterpenoids, Network pharmacology, Inflammation, Molecular docking, *In Silico* ADMET

The genus *Crataegus* (Rosaceae), commonly referred to as hawthorn, represents a rich source of natural products extensively used in Traditional Medicine for managing cardiovascular diseases[1–3]. *Crataegus* spp. are widely distributed in various regions across North America, temperate zones of Asia, Africa and North Europe comprising over 200 species[1,2]. Different plant parts, including leaves, flowers and fruits, have historically been utilized for treating cardiovascular conditions, cancer, diabetes, hyperlipidemia, cough, flu, asthma, or rheumatic pain[2,3]. Recognized as "Traditional herbal medicinal products" by the European Medicines Agency (EMA, 2016), *Crataegus* species are included in European, American, and Canadian pharmacopeias.

[1]Laboratoire de Biochimie Appliquée, Faculté des Sciences de la Nature et de la Vie, Université de Bejaia, 06000 Bejaia, Algeria. [2]Departamento de Química Orgánica, Instituto Universitario de Bio-Orgánica Antonio González, Universidad de la Laguna, Avda. Astrofísico Francisco Sánchez Nº 2, 38206 La Laguna, Tenerife, Spain. [3]Departamento de Farmacología, Farmacognosia y Botánica, Facultad de Farmacia , Universidad Complutense de Madrid (UCM), Plaza Ramón y Cajal s/n, 28040 Madrid, Spain. [4]Department of Biology, Faculty of Science, University of Amar Tlidji, 03000 Laghouat, Algeria. [5]Unidad de Terapias Farmacológicas, Área de Genética Humana, Instituto de Investigación de Enfermedades Raras (IIER), Instituto de Salud Carlos III, Carretera de Majadahonda-Pozuelo Km 2, 28220 Madrid, Spain. [6]Djoudi Boukerouis and Irene Cuadrado have contributed equally to this work. ✉email: lasheras@ucm.es; aarnesty@ull.edu.es; shortelano@isciii.es

The chemistry and pharmacological activities of *Crataegus* suggest substantial interest for future discoveries. Known bioactive molecules include flavonoids, triterpenes, oligomeric proanthocyanidins, and organic acids[2–4]. However, relatively few species have been thoroughly studied, particularly concerning their ethnobotanical and therapeutic uses in Asia and Europe. Among these, *Crataegus azarolus* L, native to the Mediterranean countries, has a longstanding medicinal use due to its diverse pharmacological properties, such as anti-inflammatory, antimicrobial, antioxidant, antihyperglycemic, and antihyperlipidemic activities[5,6]. Despite the widespread recognition of hawthorn's pharmacological properties, primarily attributed to its proanthocyanidins, flavonoids, tannins, vitamin C, and glycosides[5], research on novel bioactive compounds, particularly those with non-phenolic structures, are still limited. Notably, ursane triterpenes such as ursolic acid (1), pomolic acid (2) and corosolic acid (3) (Fig. 1), have been isolated from various *Crataegus* species, including *Crataegus azarolus* L[4,7,8]. However, there is limited evidence regarding the effects of triterpenes in this medicinal plant. Interestingly, fupenzic acid (4) (Fig. 1), an ursane triterpene, was isolated in our laboratory from the leaves of *Crataegus azarolus* L, along with other well-known triterpenes such as ursolic acid or pomolic acid. Although fupenzic acid (FA) has been previously detected in small quantities in certain *Crataegus* species[7,8], its biological activity remains largely unknown, representing a promising avenue for future research.

This study aims to address this gap by exploring the pharmacology activity of FA, focusing on its anti-inflammatory potential. Unlike previous studies, which have primarily focused on the phytochemical properties of *C. azarolus* extracts, this work search to expand the understanding of the bioactive compounds in hawthorn, highlighting the significance of non-phenolic constituents such as FA. Employing a comprehensive multidisciplinary approach, including network pharmacology, molecular docking, in vitro assays, and in silico analyses, the study uncovers novel mechanisms underlying the therapeutic effects of FA. The findings have significant implications for advancing research on *Crataegus azarolus*. This work provides valuable insights into the physicochemical properties and ADMET (absorption, distribution, metabolism, excretion, and toxicity) parameters of FA, confirming its safety and bioavailability. Furthermore, the study investigated the specificity and selectivity of FA for key molecular targets, such as NF-κB. The findings have been further validated by molecular docking and induced fit docking studies, along with additional in vitro experiments to corroborate the proposed mechanisms of action.

In summary, FA emerges as a promising candidate for the treatment of inflammation-related diseases, presenting new opportunities for therapeutic development.

Results

Network pharmacology analysis predicted the targets and potential mechanisms of fupenzic acid

Employing a network pharmacology-based strategy, we identified 272 potential targets of FA (Supplementary Table S1). In order to elucidate the biological behaviors of predictive targets, GO functional enrichment analysis, and Reactome and KEGG pathways analysis were performed using DAVID functional annotation tool. The top 10 significantly enriched terms are depicted in Fig. 2A-C. Further information on the overrepresented GO functional pathways, Reactome and KEEG can be found in Supplementary Tables S2-S4.

As shown in Fig. 2A, terms such as inflammatory response GO:0006954, protein phosphorylation GO:0006468, positive regulation of MAPK cascade GO:0043410 and response to lipopolysaccharide GO:0032496 were among the 10 highly enriched functions in the biological process (BP). As expected, among the top 10 Reactome and KEGG pathways, cytokine signaling in immune system, innate immune system, chemokine signaling pathway, pathways in cancer and PI3K-Akt signaling pathway were significantly associated with the activity of FA (Fig. 2B and C).

Interestingly, a reanalysis of the GO terms, with a specific focus on pathways involved in inflammation, using keywords such as "inflammation", "lipopolysaccharide," "nitric oxide," "toll-like receptor," and "NF-kappaB," led to the identification of 59 enriched terms associated with the inflammatory response (Supplementary Table S5). These findings highlight the critical role of inflammatory processes in the pharmacological effects of FA.

In order to explore which transcription factors may be involved in the modulation of the biological processes regulated by this compound, the transcription factor (TF)-target enrichment was predicted by using the TRRUST database. As illustrated in Fig. 2D and Supplementary Table S6, RELA, SP1 and NFKB1 emerged as the top three regulators in terms of the number of genes they target, suggesting their crucial role in the activity of FA.

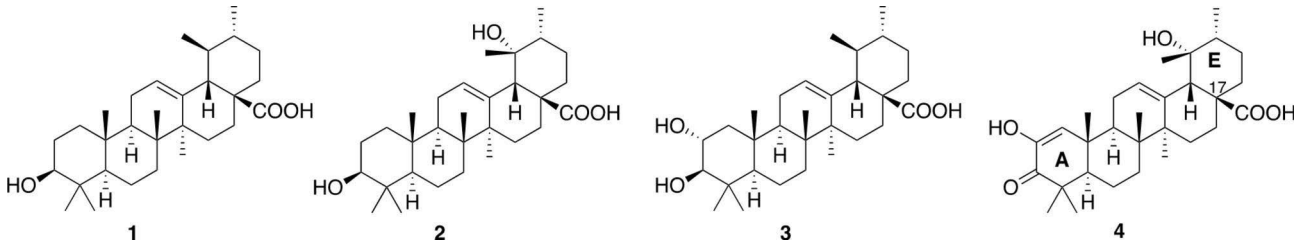

Fig. 1. Representative ursane triterpenes. (**1**) ursolic acid, (**2**) pomolic acid, (**3**) corosolic acid, (**4**) fupenzic acid.

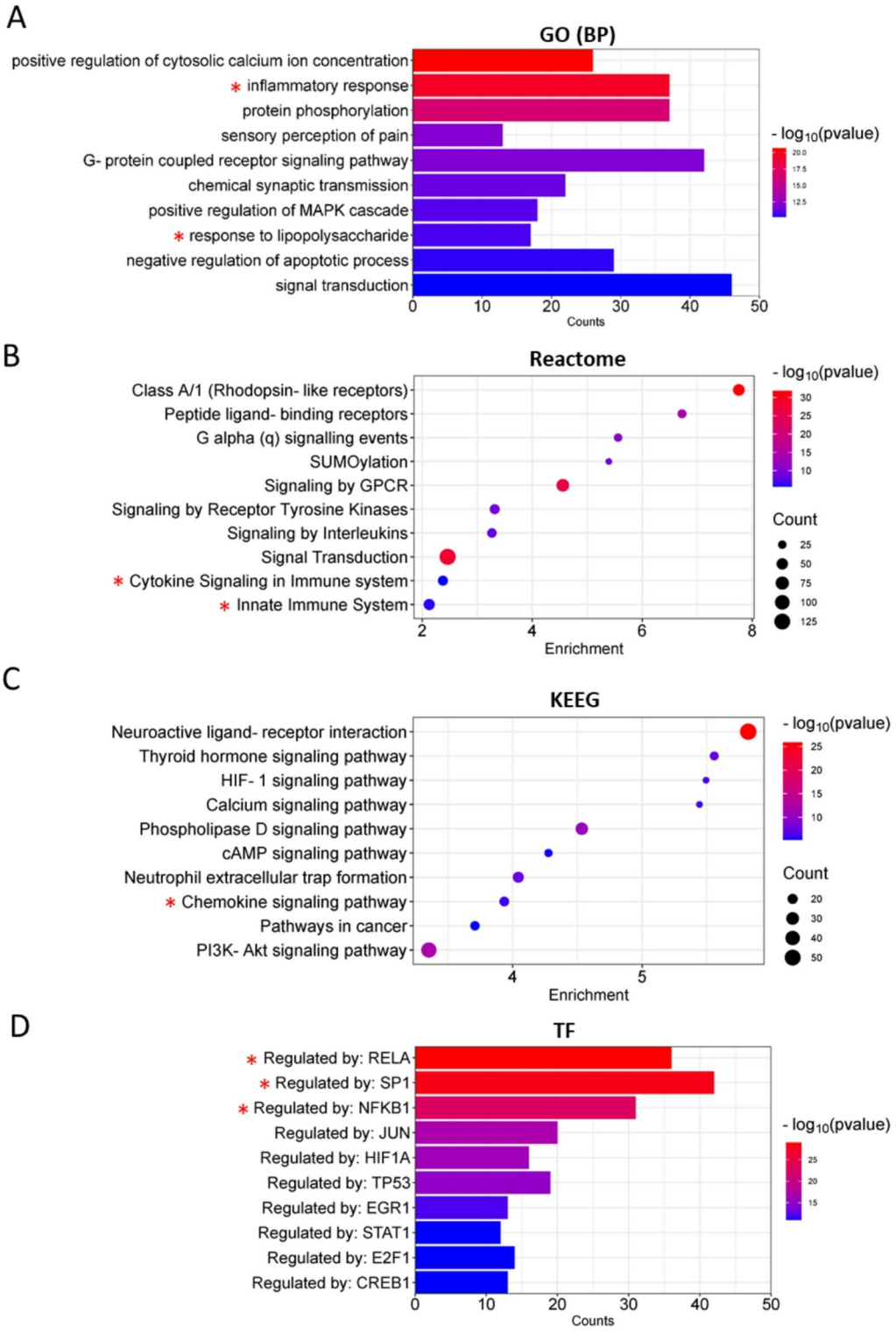

Fig. 2. GO, Reactome, KEGG and TF pathway functional enrichment analysis of potential targets for fupenzic acid. (**A**) GO functional analysis of top 10 significantly enriched biological processes (BP). The x-axis represents the number of genes involved in GO terms, and the y-axis the significantly enriched GO terms. (**B**,**C**) Dot plot of top 10 significantly enriched Reactome and KEGG pathways, respectively. The y-Axis denotes the pathway name, whereas the x-axis indicates the degree of enrichment for each of pathway. The size of the bubbles is proportional to the number of genes represented. The color bar represents the p-value. (**D**) Enrichment analysis of top 10 significantly enriched transcription factors (TF). The x-axis represents the number of genes regulated by the TF, and the y-axis the significantly enriched TF. Red asterisk indicates significant pathways. *GO* gene ontology, *KEGG* kyoto encyclopedia of genes and genomes, *TF* transcription factor.

Construction of PPI network and identification of hub targets

To further investigate the relationship between targets, PPI analysis was performed with a minimum interaction score of 0.7 (high confidence). The resulting PPI network comprised 235 nodes and 558 edges, with an average node degree of 5 and an average clustering coefficient of 0.485 (Fig. 3A). The PPI enrichment was considered significant at $p < 1.0e\text{-}16$. The PPI network was then exported to Cytoscape and analyzed through the CytoHubba plugin to identify the top 10 hub genes based on topological analysis (degree, MCC and MNC). The top 10 genes with the highest degree, MCC and MNC scores were designated as hub genes, as shown in Fig. 3B and Supplementary table S7. The intersection from the three methods was explored, and a Venn plot was generated to visualize the overlapped hub genes (Supplementary Figure S1).

Fupenzic acid did not affect cell viability

In order to validate the potential targets involved in the anti-inflammatory effects of FA, in vitro experiments were conducted. First, we assessed the viability of peritoneal macrophages cells following exposure to FA (0–50 μM), using an MTT assay. As seen in Fig. 4, the triterpene did not significantly affect cell viability at concentrations below 20 μM. Consequently, this dosage was chosen as the highest concentration for the subsequent studies.

Fupenzic acid inhibited the expression of pro-inflammatory mediators

To further investigate the anti-inflammatory potential of FA, we analyzed its effects on classical inflammation markers after stimulation with LPS. LPS, a component of the cell wall of gram-negative bacteria, can trigger the innate immune response by binding to components of the Toll-like receptor (TLR) signaling pathway, especially TLR4. The binding of LPS to TLR4 receptors on macrophages, leads to activation of the nuclear transcription factor-κB (NF-κB) signaling pathway, a crucial step in the onset of the inflammatory response. NF-κB orchertrates the expression of proinflammatory mediators and enzymes such as NOS-2 and COX-2, alongside a wide array of pro-inflammatory cytokines and chemokines. Peritoneal macrophages were pretreated with the triterpene for 30 min, followed by incubation with LPS (specific to TLR4) for 24 h. Nitric oxide (NO) release, indicative of NOS-2 activation, was assessed, revealing a dose-dependent inhibition of nitrite accumulation in the culture medium by FA (with an IC_{50} of 16.7 μM) (Fig. 5A). Further, we evaluated the activation of the pro-inflammatory genes NOS-2 and COX-2. In unstimulated peritoneal macrophages, the levels of NOS-2 and COX-2 proteins were undetectable. As expected, LPS treatment resulted in the activation of both proteins. However, upon pre-incubation with the triterpene and subsequent stimulation with LPS for 24 h, a significant inhibition of the protein expression of NOS-2 and COX-2 was observed (Fig. 5B).

The analysis of NOS-2 and COX-2 mRNA by real-time quantitative PCR demonstrated that FA inhibited LPS-induced expression of both enzymes, exerting its effects at the transcriptional level (Fig. 6). To ascertain whether the triterpene influenced other inflammatory mediators such as cytokines, we assessed levels of interleukin (IL)-6, IL-10, IL-18 and IL-12, tumor necrosis factor-α (TNF-α), interferon gamma-induced protein 10 (IP-10) and keratinocyte chemoattractant (KC). Upon stimulation with LPS, all cytokines were found to be downregulated at the mRNA level in the presence of the triterpene (Fig. 6). Interestingly, these findings underscored the broad effect of this triterpene on the transcriptional regulation of pro-inflammatory genes associated with the LPS-induced response.

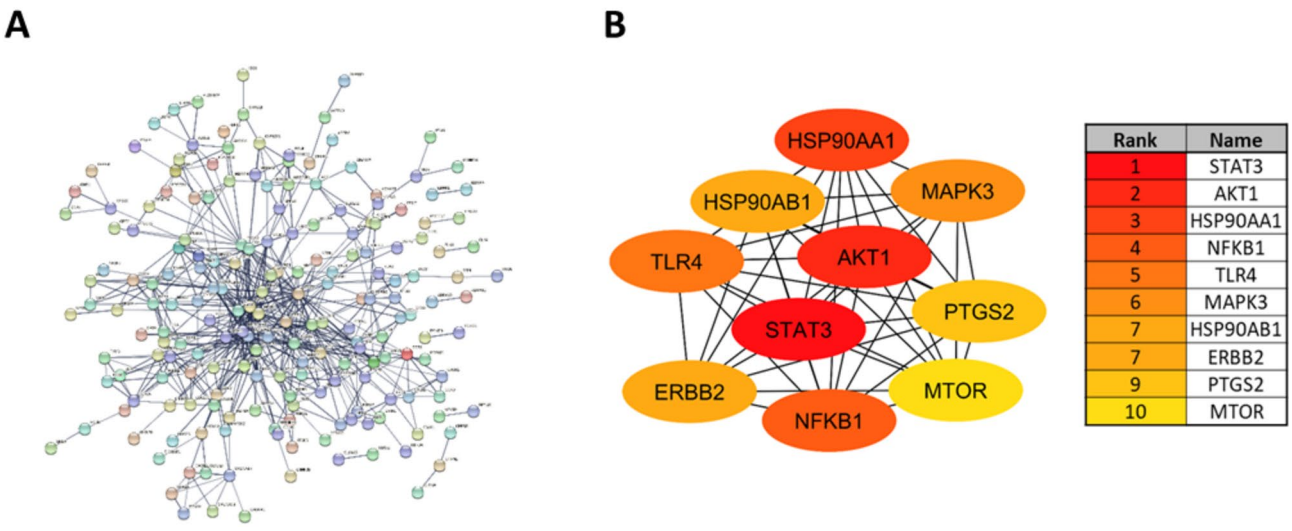

Fig. 3. PPI network integration and Hub gene identification for fupenzic acid. (**A**) PPI network of overlapping differentially expressed genes was constructed using the STRING database. (**B**) Analysis of the top 10 hub targets networks by the degree algorithm, with red and yellow representing the importance of the nodes within the network.

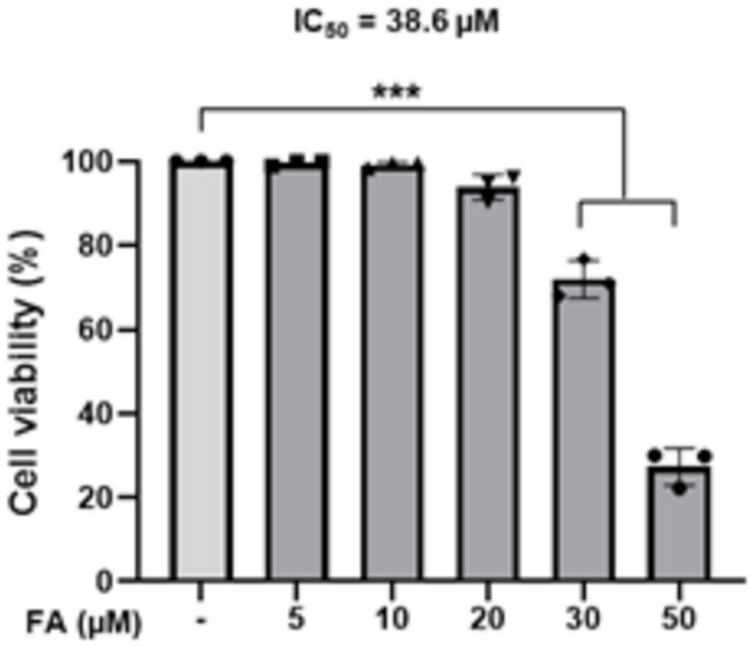

Fig. 4. Cell viability after treatment with fupenzic acid. Peritoneal macrophages were treated with 5, 10, 20, 30 or 50 µM of fupenzic acid (FA) for 24 h. Cell viability was determined by the MTT assay. Results are reported as mean of cell viability (% of non-treated cells) of at least three independent experiments ± SD. *** $p < 0.001$ vs. non-treated cells.

Fupenzic acid modulated NF-κB activation

The activation of NF-κB depends on the phosphorylation and subsequent degradation of inhibitory kappa B (IκB) proteins, which results in the translocation of p65/p50 heterodimers to the nucleus. Therefore, the subsequent objective was to ascertain whether the anti-inflammatory effect of the triterpene could be ascribed to its inhibitory effects on this pathway. As shown in Fig. 7, degradation of IκBα and IκBβ was impaired in LPS-activated macrophages pretreated with FA. Furthermore, a notable reduction in the accumulation of the NF-κB p65 subunit in the nucleus was observed after treatment with the triterpene.

Molecular docking studies

Based on the in vitro experiments and the identification of hub core genes by network pharmacology, the transcription factor NF-κB emerges as a pivotal target for the action of FA. Consequently, we conducted molecular docking studies to elucidate mechanistic details of the interaction between FA and NF-κB, as well as rationalize the observed biological outcomes. In the absence of a 3D structure of NF-κB in complex with a small-molecule inhibitor, the Site Finder module of the Molecular Operating environment (MOE) suite of programs was employed for the identification of potentially druggable surface sites on the X-ray crystal structure of a NF-κB (PDB 2O61). MOE's Site Finder is a geometric method used to calculate potential active sites in a receptor from its 3D atomic coordinates and rank the sites according to their Propensity for Ligand Binding (PLB) score, which is based on the amino acid composition of the pocket[9]. The hypothetical ligand binding site of the NF-κB transcription factor is located between the two domains of the protein overlapping with the DNA-binding site (Fig. 8).

It is worth highlighting that the loop that connects the protein domains to stabilize its interaction with DNA, is due to the presence of amino acids with positively charged nitrogen that interact specifically with the DNA bases and non-specifically with the phosphate groups by the formation of ionic interactions. NF-κB dimers use flexible loops to mediate contacts with DNA rather than using α- helices as often observed in other transcription factors[10]. Therefore, any type of interaction that our ligand might have with positively charged amino acids present in DNA binding site, could play an important role in the inhibition of the NF-κB-DNA complex. Hence, FA was docked into the predicted ligand binding site on NF-κB surface with the aim of seeing if it is able to interact properly with this target and, consequently, to elucidate the potential binding mode and key active site interactions.

As expected, these docking results strongly suggested that the compound shows a good steric and electronic complementarity into the predicted ligand binding site on NF-κB. Furthermore, an analysis of them revealed that most of the best docking poses obtained during the simulation showed hydrogen bond interactions with positively charged amino acids located within the DNA binding site. In the predicted pose of FA [(4), see Fig. 1)], three hydrogen bonds were detected, two of them between the residues of Arg35 and Arg33 and the carbonyl and hydroxyl groups present in ring **A**. Likewise, another hydrogen bond can be observed between the Gly31 residue, and the hydroxyl group found in the **E** ring. Additionally, there are also numerous potential hydrophobic

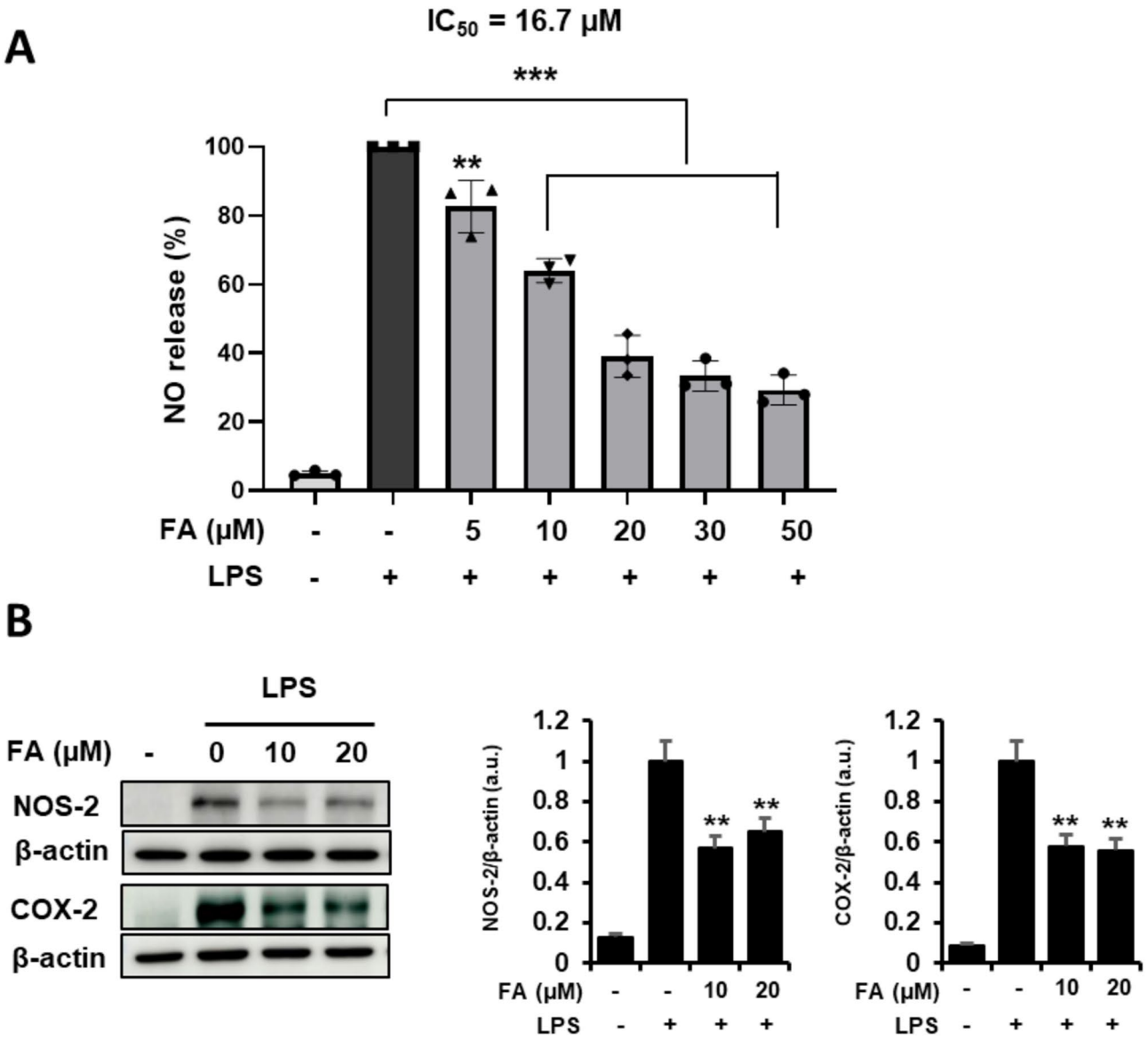

Fig. 5. Effects of fupenzic acid on inflammatory mediators. (**A**) Peritoneal macrophages were preincubated with fupenzic acid (FA) (5, 10, 20, 30 and 50 µM) followed by stimulation with 1 µg/ml LPS (TLR4 ligand) for 24 h. Nitrite accumulation in the culture medium was quantified using the Griess reagent and expressed as the percentage of NO release compared to LPS treatment. (**B**) Macrophages were preincubated for 30 min with the compound (10 and 20 µM) followed by stimulation with 1 µg/ml LPS (TLR4 ligand) for 24 h. NOS-2 and COX-2 proteins were detected by Western blot. β-actin was used as a loading control. Experiments were carried out in triplicate and results show the mean ± SD. $^{**}p < 0.01$ and $^{***}p < 0.001$ vs. LPS-treated cells.

interactions involving residues such as Gly44, Ser51, ASP53, Glu193, Met32, Pro47, Ala 43, and Arg35 (Fig. 9). On the other hand, depending on the conformation obtained during the molecular docking simulation, two other hydrogen bonds interactions can also be observed between the Lys28 and Ser51 residues and the carbonyl group at **C-17**. Therefore, hydrogen bonds interactions formed with the positively charged residues Arg35 and Arg33 of the NF-κB protein play a dominant role on the anti-inflammatory activity of FA) by inhibiting the transcription factor NF-κB. The free binding energy for the best binding mode of compound was an S score value of − 6.08 kcal.mol^{-1} after applying induced fit calculation as a refinement method and GBVI/WSA dG as the final scoring methodology.

Drug-likeness and oral-bioavailability analysis of fupenzic acid

Physicochemical and drug-likeness parameters of FA, including topological polar surface area (TPSA) and bioavailability, are shown in Table 1. It met all the criteria of Lipinski's rule with no violations. Other properties such as the solubility (Log S and XLOGP3) and the fraction of sp3 carbons are also included. Finally, the bioavailability score was also calculated, revealing that FA had acceptable bioavailability score (0.56).

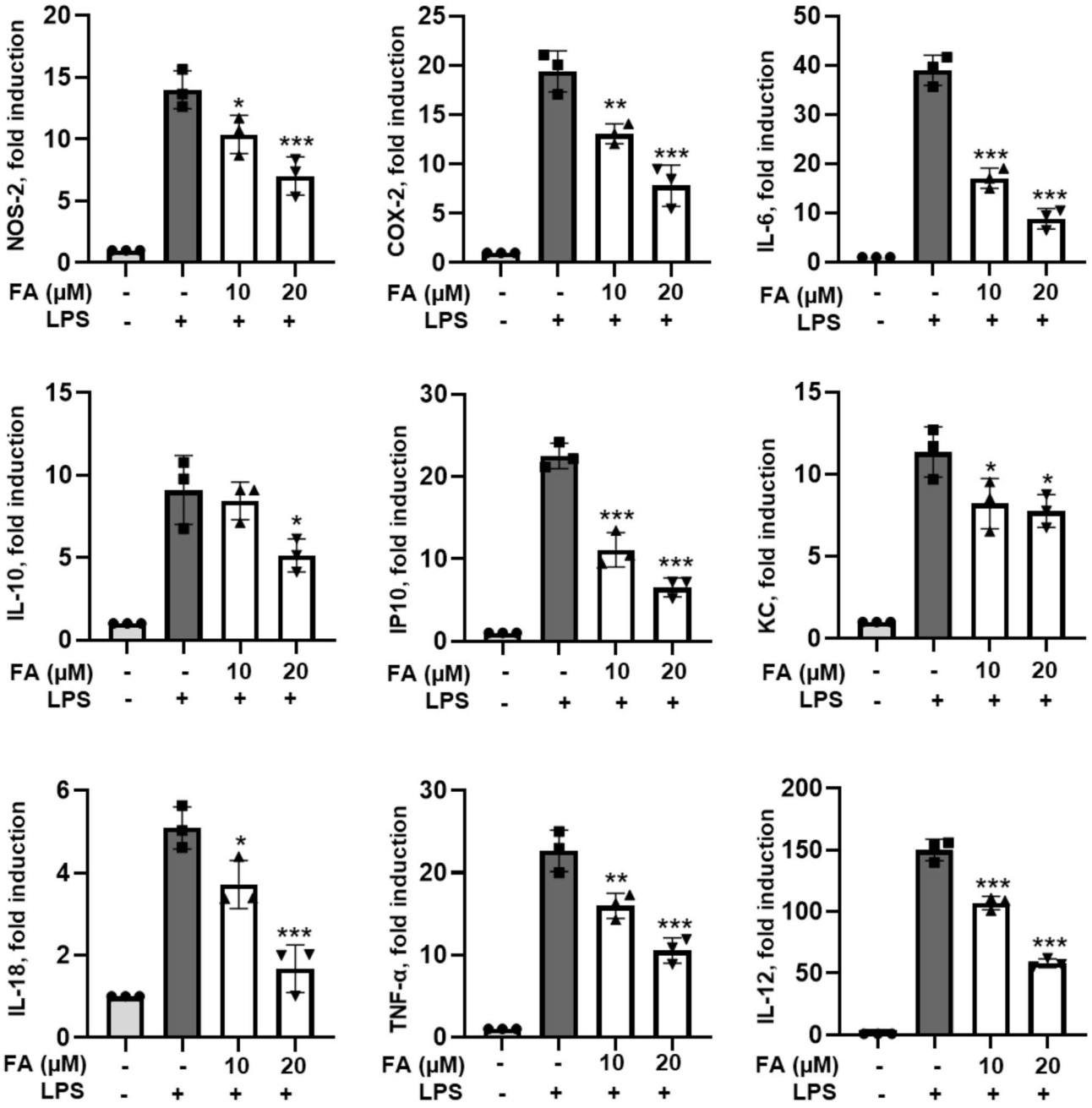

Fig. 6. Pro-inflammatory gene expression is inhibited by fupenzic acid. Mouse peritoneal cells were pre-treated with fupenzic acid (FA) (10 and 20 μM) for 30 min and then stimulated during 6 h with 1 μg/ml of LPS-TRL4 specific ligand. RT-PCR experiment was performed to amplify RNAm corresponding to: NOS-2, COX-2, IL-6, IL-10, IL-12, IL-18, KC, TNF-α, and IP-10. Results are expressed as fold changes relative to LPS (TLR4 ligand) treated cells. $^{*}p < 0.05$, $^{**}p < 0.01$, and $^{***}p < 0.001$ vs. LPS-stimulated cells.

Assessment of ADMET properties

The prediction of ADMET properties is of critical importance in ensuring the overall efficacy and safety of novel therapeutic molecules. Therefore, pharmacokinetic properties were also calculated using pkCSM server (Table 2).

Drug absorption depends on various factors, including water solubility, GI (gastrointestinal) absorption, membrane permeability [as evidenced by the colon cancer cell line (Caco-2)], and skin permeability levels. FA was predicted to be moderately soluble in water and demonstrated robust GI absorption (> 30%). However, its Caco-2 membrane permeability was assessed as low (log Papp value < 0.9 cm/s), and skin permeability fell below the standard threshold (log kp ≥ − 2.5 cm/s), suggesting limited absorption potential through the skin. Additionally, the prediction of P-glycoprotein non-substrate drug candidates is crucial in absorption analysis. FA was identified as substrate for P-gp, implying a potential impact on its absorption and distribution within

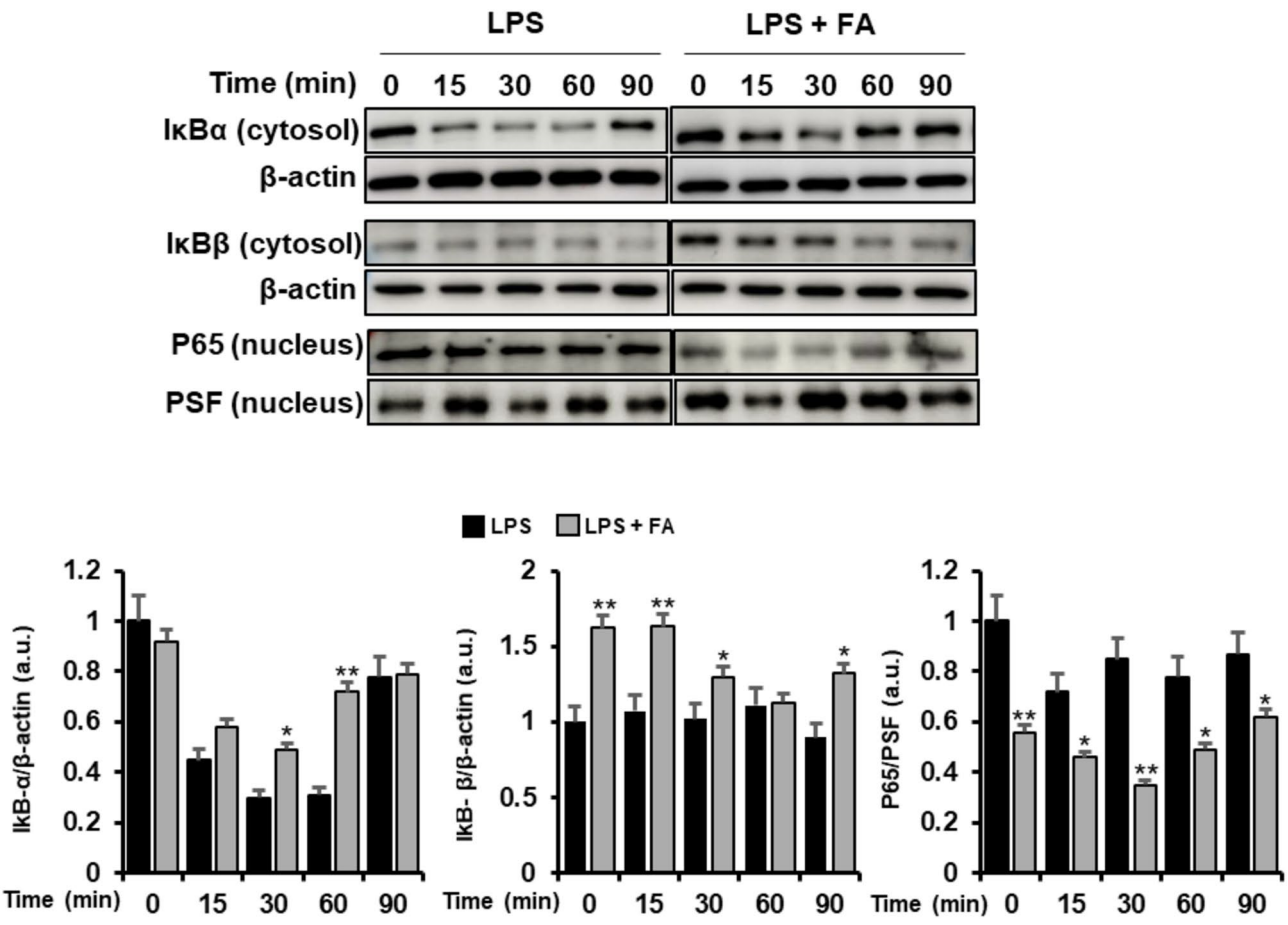

Fig. 7. Fupenzic acid inhibits NFκB activation. Peritoneal macrophages were pre-treated for 30 min with fupenzic acid (FA) (20 μM) and then activated for the indicated times with 1 μg/ml LPS (TLR4 ligand). The levels of IκBα and IκBβ (cytosolic extracts) and p65 (nuclear extracts) were determined by Western blot. β-actin and PSF were used as a loading control. $^{*}p < 0.05$, and $^{**}p < 0.01$ vs. LPS-stimulated cells.

the body. Furthermore, the ability of FA to permeate and distribute across various physiological barriers was examined, including distribution volume (VDss), central nervous system (CNS) permeability and blood–brain barrier membrane permeability (logBB). Results indicated a low VDss for FA (LogVDss less than − 0.15 is considered to have a small volume of distribution in tissues), suggesting minimal distribution in tissues and mitigating the risk of renal failure and dehydration. Moreover, its logBB value suggested poor BBB permeability, indicating limited ability to cross the blood-brain barrier and negligible penetration of the CNS. This feature could potentially mitigate CNS toxicity risks.

Regarding drug metabolism in liver, cytochrome P450 plays a fundamental role with different cytochrome P450 isoenzymes involved such as CYP1A2, CYP2C19, CYP2C9, CYP2D6, CYP3A4. In silico studies revealed no inhibitory activity of FA on any isoform, implying its facile metabolism and consequent bioavailability post-oral administration, thus reducing the likelihood of adverse effects such as toxic accumulation or drug interactions. Excretion profile of a molecule is predicted based on two major properties: total clearance and Renal organic cation transporter 2 (OCT2) substrate identification. Fupenzic acid was not predicted as substrate for the renal OCT2 and displayed a total clearance score < 0.1. Finally, a key concern in drug development is toxicity studies, since the selected drug candidates must demonstrate not only high activity but also low toxicity. Our results show that FA showed no mutagenicity in AMES toxicity assays and did not trigger alerts as a Pan Assay Interference compound (PAIN), suggesting suitability for in vivo assays to assess its activity. Besides, it had no inhibitory effect on hERG1, thereby reducing the risk of cardiotoxicity, and had no discernible effect on the skin.

According to these findings, the proposed compound has a good pharmacological profile and could potentially be an efficient anti-inflammatory drug.

Discussion

The findings of this study offer valuable insights into the pharmacological potential of *Crataegus azarolus* L., with a particular focus on the bioactivity of FA, an ursane triterpene with limited previous characterization. The relationship between the pharmacological activity and specific compounds of *Crataegus azarolus* L. remains insufficiently understood, and there is a notable lack of studies addressing its toxicological profiles

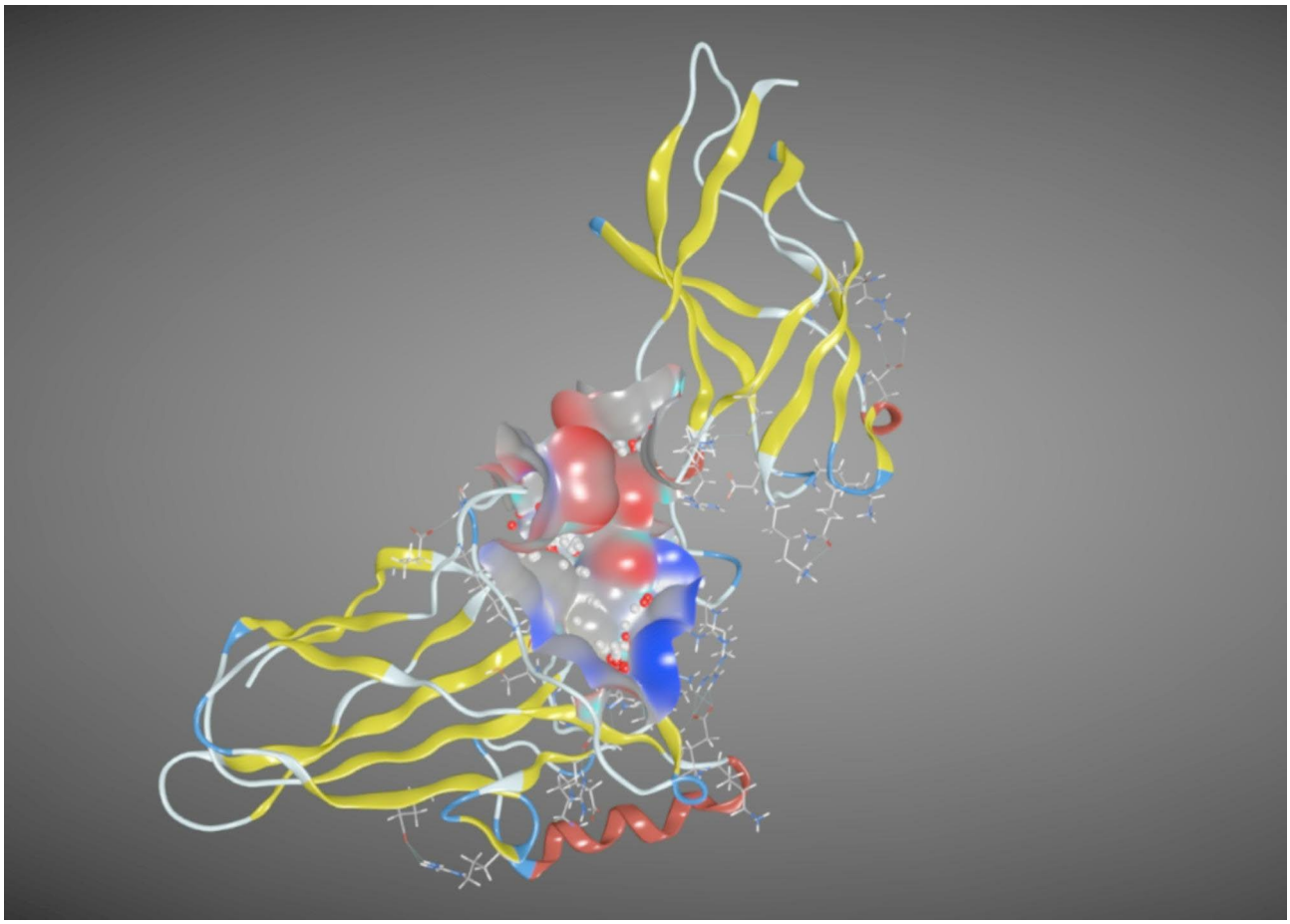

Fig. 8. Predicted binding site obtained by MOE's Site Finder and used for the molecular docking simulation into the NF-κB protein.

and pharmacokinetic properties. This study highlights the key therapeutic targets and potential mechanisms of FA. By using network pharmacology, an innovative approach that enhances drug screening efficiency[12], we have identified 272 potential targets for FA. Bioinformatics analyses, including GO, KEGG pathway, and PPI network assessments, revealed strong associations between these targets and key inflammatory processes such as cytokine and chemokine signaling, innate immune responses, protein phosphorylation, and lipopolysaccharide-induced activation. Notably, NF-κB emerged as a pivotal target of inflammation. To the best of our knowledge, this is the first study to explore the therapeutic targets and signaling pathways associated with FA, with particular emphasis on its interaction with NF-κB.

Inflammation is a tightly regulated process orchestrated by the immune system in response to injury or infection. Nevertheless, its dysregulation contributes to the pathogenesis of various diseases, including cancer, cardiovascular disease, diabetes mellitus, obesity, ulcerative colitis, or pulmonary disorders[13]. Among immune cells, macrophages play a central role in the inflammatory response by synthesizing and releasing key pro-inflammatory mediators, such as reactive oxygen and nitrogen metabolites, eicosanoids, chemokines, and cytokines[14,15]. Consequently, suppression of the inadequate inflammatory responses is essential for managing these pathologies, underscoring the need to identify novel anti-inflammatory compounds.

Natural products have long been a valuable source of bioactive compounds owing to their broad pharmacological activities[16]. *Crataegus* spp., including *Crataegus azarolus* L., possess a rich chemical composition comprising polyphenolic compounds, organic acids and triterpenes, many of which have demonstrated anti-inflammatory properties[2,3]. From the leaves of *C. azarolus L*, we have isolated several pentacyclic triterpenes including ursane triterpenoids (uvaol, ursolic acid, 11-oxo-ursolic acid, 2α,19α-dihydroxy-3-oxo-urs-12-en-28-oic acid, pomolic acid, 2-oxopomolic acid, euscaphic acid, tormentic acid, azarolic acid, and fupenzic acid), oleanane triterpenoids (oleanolic acid, maslinic acid and arjunic acid) and one lupane (alphitolic acid). While many of these compounds have been studied for their anti-inflammatory and antioxidant effects, the biological activity of FA remains largely unexplored. Our study revealed that FA shares pharmacological properties with other ursane triterpenes, such as ursolic, corosolic and pomolic acid, which exhibit anti-inflammatory, antioxidant, and antihyperglycemic effects[17–19]. Experimental findings confirmed that FA plays a key role in the regulation of the inflammatory processes, which was consistent with network pharmacology predictions.

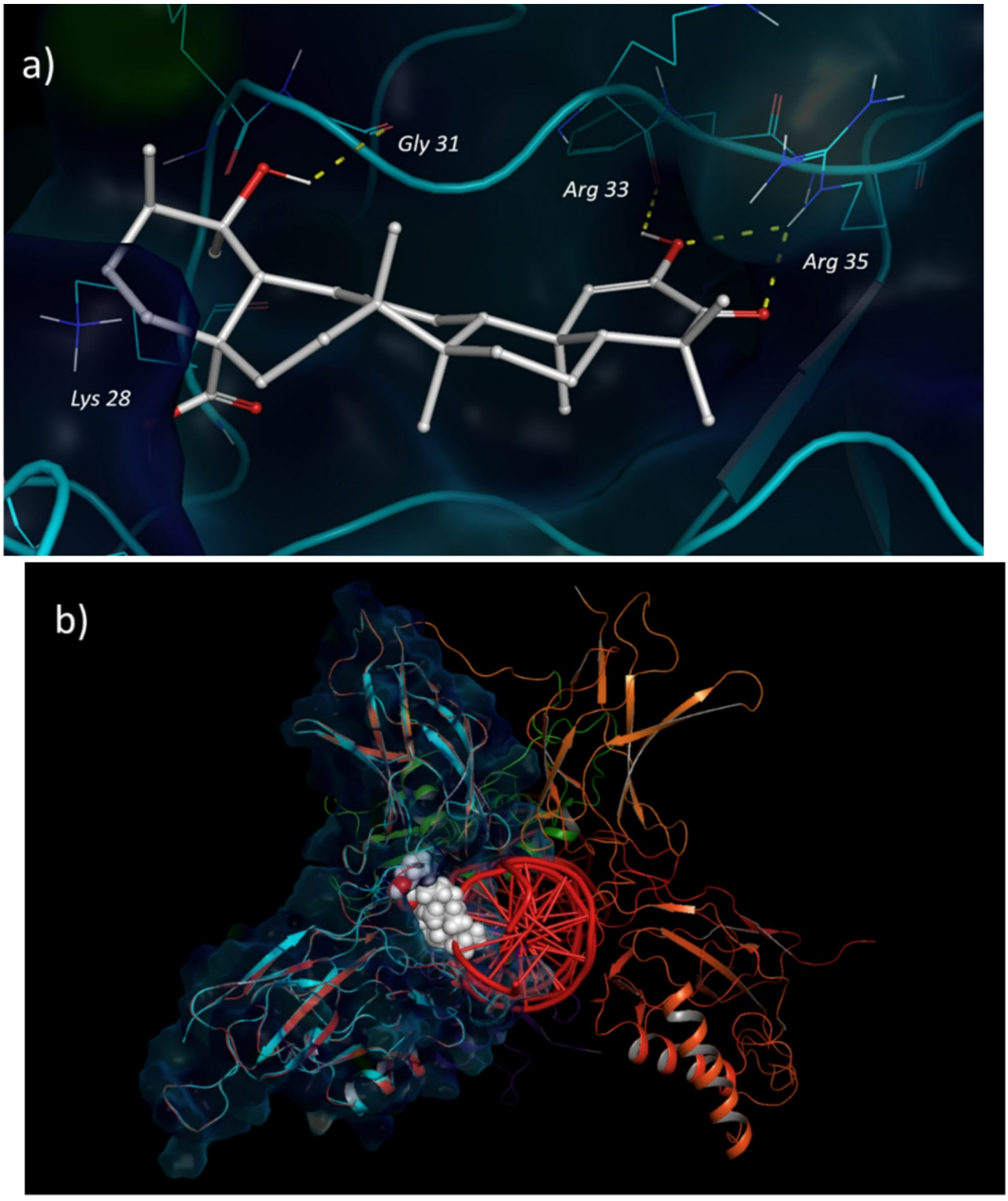

Fig. 9. (**a**) Predicted binding mode of FA and predicted ligand binding site on NF-κB. (**b**) Alignment of the best docking pose of FA on the Crystal Structure of NF-κB, where the interactions located within the DNA binding site are observed and visualized through PyMol Software v2.5.8[11].

Specifically, FA suppressed the production of NO in LPS-induced macrophages, and inhibited the expression of NOS-2, COX-2, and other inflammatory mediators, including IL-6, IL-10, IL-12, IL-18, KC, TNF-α, and IP-10.

NF-κB was identified in our analysis as a primary target of FA. Activation of NF-κB triggers the transcription of various proinflammatory mediators, including NOS-2, COX-2, chemokines and cytokines, all of which contribute to the inflammatory response[20]. It is noteworthy that this transcription factor represents a common

Molecular weight (g/mol) ≤ 500	484.67
H-bond acceptors (nHBA) ≤ 10	5
H-bond donors (nHBD) ≤ 5	3
LogP (lipophilicity octanol/water) ≤ 5	4.73
Lipinski's violations ≤ 1	0
Number of rotatable bonds (nRB) ≤ 10	1
Topological polar surface area (TPSA) ≤ 140 Å^2	94.83 Å^2
Aqueous solubility (Log S) ≤ 6	-6.34
XLOGP3 (-0.7–5)	5.66
Fraction Csp3 (0.5-1)	0.8
Bioavailability score	0.56

Table 1. Physicochemical parameters for fupenzic acid.

	Properties	Predicted value	Range values
Absorption	Water solubility (log mol/L)	-3.498	Moderately soluble <-4
	Caco2 permeability (log Papp in 10 –6 cm/s)	0.603	High > 0.9
	GI absorption (% Absorbed)	79.028	Poor absorbed: <30%
	Skin permeability (log Kp in cm/s)	-2.735	Low permeability: logKp > −2.5
	Bioavailability	0.56	
	P-glycoprotein substrate	Yes	
	Pgp I & II inhibitor	No	
Distribution	BBB permeant (logBB)	-0.7	Low: logBB < −1; High: logBB > 0.3
	CNS permeant (log PS)	-1.516	Penetrate is > −2, Unable is < − 3
	VDss (human) (log L/Kg)	-1.2	Low: log VDss < −0.15, High: log VDss > 0.45
Metabolism	CYP1A2 inhibitor	No	
	CYP2C19 inhibitor	No	
	CYP2C9 inhibitor	No	
	CYP2D6 inhibitor	No	
	CYP3A4 inhibitor	No	
Excretion	Total Clearance	-0.096	High (> 1 mL/min/kg), medium (> 0.1 to < 1 mL/min/kg), or low (≤ 0.1 mL/min/kg)
	Renal OCT2 substrate	No	
Toxicity	AMES toxicity	No	
	hERG I inhibitor	No	
	hERG II inhibitor	No	
	Skin Sensitisation	No	
	PAINS #alerts	0	

Table 2. Prediction of ADMET properties.

target in the mechanism of action of terpenes[21,22]. Thus, several triterpenes have been identified as NF-κB signaling inhibitors, interfering with the nuclear translocation of NF-κB, inhibiting its DNA-binding, and blocking the transcription of cytokines and other pro-inflammatory proteins[23–27]. Consistent with these findings, PPI network analysis highlighted NF-κB as a key target of FA. Furthermore, in vitro experiments demonstrated that FA modulates the IκBs/NF-κB signaling by reducing the phosphorylation of IκBα and IκBβ and preventing the nuclear translocation of NF-κB p65 in LPS-activated macrophages, thereby resulting in decreased pro-inflammatory cytokine production. Molecular docking analysis further confirmed strong binding interactions between FA and NF-κB, reinforcing the likelihood that anti-inflammatory activity of FA is mediated through inhibition of this pathway.

Although the inhibition of NF-κB signaling emerged as a central finding, other pathways identified in our analysis may also contribute to the anti-inflammatory activity of FA. For instance, the MAPK signaling cascade was highlighted as another critical mediator of inflammation. MAPKs play a key role in transmitting extracellular signals to intracellular responses, regulating the production of pro-inflammatory cytokines and enzymes such as COX-2. Indeed, our findings align with previous studies on triterpenes, including ursolic acid, oleanolic acid, and pomolic acid, which have been reported to inhibit NF-κB and MAPK signaling[18,23,28]. Additionally, cytokine signaling, innate immune responses, and LPS response, were also recognized as relevant targets. These pathways are integral to the activation and regulation of immune cells, particularly macrophages, which play a central role in orchestrating inflammatory responses. Thus, FA may exhibit a broader spectrum of anti-inflammatory effects than initially anticipated.Therefore, identification of NF-κB as a primary target for FA, along with its ability to

inhibit NOS-2 and COX-2 expression and suppress pro-inflammatory cytokines, provides novel insights into its pharmacological potential, underscoring its functional similarity to other bioactive triterpenes.

Finally, some physicochemical and ADMET parameters were estimated to predict its oral bioavailability and minimize potential toxicity risks. The results show that FA satisfied the principles of Lipinski's 'rule of five', suggesting favorable absorption following oral administration. ADMET prediction assessments underscored FA's minimal toxicity (non-carcinogenic, absence of AMES or cardiac toxicity), alongside favorable intestinal absorption and a high bioavailability score. Furthermore, the compound displayed low BBB permeability, minimizing the risk of unwanted CNS-related side effects. Nevertheless, ADMET analysis also suggested poor skin permeability and low tissue distribution, which contrasts with its compliance with Lipinski's 'rule of five' and its high bioavailability score. This apparent discrepancy could be attributed to several factors, including the involvement of alternative absorption mechanisms or selective tissue accumulation. For instance, FA could exhibit enhanced bioavailability when co-administered with other phytochemicals from *Crataegus azarolus*, such as flavonoids or proanthocyanidins, known to modulate pharmacokinetics. Furthermore, standard in silico models might underestimate its bioavailability, as they do not account for complex biological interactions.

In summary, while in silico and in vitro findings provide compelling evidence for the therapeutic activity of FA, experimental validation will be required to confirm their biological relevance and therapeutic applicability in vivo models.

Conclusion

The anti-inflammatory potential of *Crataegus* spp. has been widely attributed to their wide phytochemical composition, including polyphenols and organic acids. FA adds to this repertoire as a novel compound with specific activity against NF-κB-mediated pathways. Our study highlights the anti-inflammatory potential of FA, demonstrating its ability to modulate NF-κB signaling and suppress pro-inflammatory mediators in macrophages. By bridging in silico predictions with experimental validation, our work underscores the value of integrating computational and experimental approaches in drug discovery. The findings provide compelling evidence supporting the role of FA as a novel new anti-inflammatory agent and emphasize it as a noteworthy candidate for further investigation.

Materials and methods

Plant material

Leaves of *Crateagus azarolus* L were collected in June 2014 from the hills of Tala ighil province of Sidi Ayad, Bejaia (Algeria) (the Global Positioning Systems (GPS) location is 36.644 °N 4.921 °E). The plant was identified in the Department of Botany, University of La Laguna, (Spain) according to a voucher herbarium specimen (code TFC 52.916).

The dried powdered leaves (800 g) were sequentially extracted using hexane, dichloromethane, (DCM), and methanol (MeOH) in a Soxhlet apparatus, yielding 14.6 g of hexane extract, 11.44 g of DCM extract, and 28.7 g of MeOH extract. The DCM extract was fractioned by vacuum liquid column chromatography on silica gel 60 (0.2–0.5 mm) and eluted with mixtures of n-hexane/EtOAc of increasing polarity. Six fractions, designated A (0.12 g), B (0.44 g), C (2.17 g), D (0.72 g), E (0.70 g) and F (1.08 g), were separated and further chromatographed on Sephadex LH-20 and Si gel, using a mixture of n-hexane/CH_2Cl_2/MeOH (2:1:1) and n-hexane/EtOAc, respectively, as the solvents. Some of the eluted products were further purified by preparative-TLC. Fraction A yielded uvaol[29] 37.4 mg). Fraction B gave a main subfraction B-2 (253 mg) containing a mixture of ursolic acid[30] and oleanolic acid[31] difficult to separate. Fraction C yielded uvaol[29] (27.5 mg), ursolic acid[30] (44.1 mg), 11-oxo-ursolic acid (4.3 mg)[32], oleanolic acid[31] (34.5 mg), 2-oxopomolic acid[33] (4.1 mg), 2α,19α-dihydroxy-3-oxo-urs-12-en-28-oic acid[34] (24.4 mg). Ursolic acid[30] (29.6 mg), pomolic acid[35] (32.4 mg), fupenzic acid[36] (7.3 mg) and alphitolic acid[37] (5.3 mg) were isolated from the fraction D. Fraction E afforded ursolic acid[30] (24.6 mg) and euscaphic acid[38] (28.1 mg). The last fraction F yielded tormentic acid[39] (4.6 mg), euscaphic acid[38] (14.6 mg), azarolic acid[40] (31.2 mg), maslinic acid[41] (9.4 mg) and arjunic acid[42] (2.6 mg).

Prediction of putative targets of fupenzic acid

Spectroscopic data of Fupenzic acid are included in as Supplementary Materials (Supplementary Figure S2). Canonical SMILES and chemical structural formulae of fupenzic acid (**4**) (Fig. 1) were retrieved from Pubchem (https://pubchem.ncbi.nlm.nih.gov/). SwissTargetPrediction (http://www.swisstargetprediction.ch/)[43], SuperPred3 (https://prediction.charite.de/)[44], and Targetnet (http://targetnet.scbdd.com/) databases[44] were used to identify potential target genes for fupenzic acid. Targets with a probability > 0.1 were selected from SwissTargetPrediction and TargetNet, while for SuperPred, known strong binders with a probability > 50% were included. The gene list of the targets obtained was standardized using UniProtKB database (https://www.uniprot.gov/) and any unmatched genes were removed.

Functional and pathway enrichment analysis of the predicted targets

Kyoto Encyclopedia of Genes and Genomes (KEGG), Gene Ontology (GO), and Reactome pathway enrichment analyses of the predicted targets were performed using the Database for Annotation, Visualization, and Integrated Discovery (DAVID; https://david.ncifcrf.gov)[46,47]. Pathways and terms with p-values less than 0.05 were prioritized to ensure robustness and highlight significant results. The results were ranked based on both p-value and count value, with the top 10 pathways highlighted. Furthermore, fold enrichment values were incorporated to underscore the significance of each pathway. Lastly, enrichment analysis of associated transcription factors was performed using the TRRUST v2 database (https://www.grnpedia.org/trrust/)[48].

Protein-protein interaction (PPI) network and identification of hub targets

The functional associations among the identified targets were investigated using the Search Tool for the Retrieval of Interacting Genes and proteins database (STRING) 12.0 (https://www.string-db.org/)[49] to gather protein-protein interaction (PPI) data. A PPI network was constructed with a confidence score threshold set at > 0.7. Subsequently, the network data was imported into Cytoscape 3.9.1 (https://cytoscape.org/) for visualization and further analysis. The CytoHubba plugin[49] was employed to extract network topology parameters, with hub genes identified based on their degree of connectivity, maximal clique centrality (MCC), and maximum neighborhood component (MNC). The top 10 genes were designated as hub genes and visually represented in the network according to their importance using a color scale ranging from red (most important) to yellow (less important). Overlapping hug genes were determined using Venn diagram analysis the online tool (http://bioinformatics.psb.ugent.be/webtools/Venn/)[51].

Isolation of peritoneal macrophages and cell culture conditions

All animal care and experimental protocols adhered to the European Union guidelines (EEC Directive of 1986; 86/609/EEC) and the principles of the Declaration of Helsinki principles for Animal Care. These regulations are enforced through Spanish law (RD 53/2013). The protocols were approved by the institutional animal care and use committee (IACUC) of the Instituto de Salud Carlos III (PROEX 092/17). All efforts were made to minimize animal suffering and to reduce the number of animals used. This study is reported in accordance with ARRIVE guidelines. Peritoneal macrophages were obtained from male BALB/c mice aged 8–10 weeks, from Charles River Laboratories, certified to be free of pathogens, following established procedures[51]. Briefly, mice were maintained in a pathogen-free environment and received an intraperitoneal (i.p.) injection of 1 ml of sterile 10% thioglycolate broth four days before use. Mice were anesthetized and sacrificed using CO_2. Peritoneal macrophages were then isolated by administering a 10 ml i.p. injection of sterile DMEM. The peritoneal fluid was gently aspirated to avoid hemorrhage and stored at 4 °C to prevent macrophage adherence to plastic surfaces. The cell pellet was then centrifuged at 200 × g for 10 min at 4 °C, followed by two washes with 45 ml of ice-cold PBS. Cells were subsequently seeded at a density of 1×10^6 cells/cm² in DMEM containing 10% fetal calf serum (FCS). After 2 h, nonadherent cells were removed through extensive washing with medium.

Cell viability

Peritoneal macrophages were seeded into 96-well plates and incubated with various concentrations of fupenzic acid for 24 h. Cell viability was determined using 3-(4,5-dimethylthiazol-2-yl)-2,5-diphenyltetrazolium bromide dye (MTT, 2 mg/mL, Sigma) as previously described[52]. Each assay was conducted in triplicate. The results were expressed as the percent reduction in cell viability compared to untreated controls, and were obtained from at least three independent experiments.

Determination of nitric oxide (NO) production

Peritoneal macrophages were seeded into a 96-well plate at a density of 10^5 cells per well and treated with varying concentrations of fupenzic acid (0–50 µM) for 30 min. The cells were then stimulated with 1 µg/ml of ultrapure lipopolysaccharide from *Escherichia coli* 0111:B4 (LPS specific to Toll-like receptor 4 TLR4, Invivogen) for 24 h, while continuing the treatment with the compounds for 24 h. The concentration of nitrite in the supernatants was determined using the Griess reagent (1% sulfanilamide in 5% phosphoric acid and 0.1% naphtylethylenediamine dihydrochloride) (Sigma), in accordance with established protocols[52].

Preparation of cytosolic and nuclear protein extracts and Western blot analysis

Cytosolic and nuclear proteins were extracted using a previously described protocol[52] and Western blot analysis was performed. Proteins were loaded on 6–10% SDS-polyacrylamide gels for electrophoresis and transferred to a Hybond™-PVDF membrane after separation. Membranes were blocked for 60 min with (5%: W/V) BSA or skim milk in PBS/Tween-20 (0.1%), before immunoblotting overnight at 4 °C with primary antibodies against anti-NOS-2, anti-COX-2, anti-IκBα, anti-IκBβ, anti-p65 (Santa Cruz), anti-β-actin, anti-PSF (Sigma) and both phosphorylated and non-phosphorylated forms of MAPKs: p38, JNK and ERK1/2 (Cell Signaling). The blots were then washed three times with PBS/Tween-20 and incubated with HRP-conjugated secondary antibodies for 1 h at 37 °C. Blots were developed using ECL according to the manufacturer's instructions (Cytiva). The protein levels were analyzed with ImageJ (FIJI) software 1.54f (https://imagej.net/software/fiji/downloads) and normalized to their respective controls. Uncropped full-length Western blot images for Figs. 5 and 7 are provided in Supplementary Materials as Figure S3.

RNA extraction and real-time PCR

RNA was extracted from cells using Trizol reagent (Invitrogen, Waltham, MA, USA) and reverse-transcribed into cDNA with M-MLV reverse transcriptase (Invitrogen, 28025-013). Quantitative PCR analysis was conducted using SYBRgreen on a StepOnePlus System (Applied Biosystems, Waltham, MA, USA). All samples were analyzed in duplicate, with 36B4 (acidic ribosomal phosphoprotein P0) serving as the endogenous control to normalize target gene expression levels. Relative gene expression was calculated using the 2-ΔΔCT method. Primer sequences are provided in Table 3.

Molecular docking studies

Docking simulations were performed employing Molecular Operating Environment (MOE) software package version 2020.02[9], Chemical Computing Group, Montreal, Canada. The crystal structure of NF-κB, IRF7, IRF3 bound to the interferon-β enhancer (PDB: 2O61, **Resolution**: 2.80 Å) were obtained from the protein data bank. Initially, all protein structures were prepared by adding hydrogen atoms followed by removal of water molecules

Gene	Forward primer 5'-3'	Reverse primer 5'-3'
NOS-2	GAGCTGGGCTGTACAAACCTT	CATTGGAAGTGAAGCGTTTCG
COX-2	GCTGTACAAGCAGTGGCAAAG	GCGTTTGCGGTACTCATTGAGA
IL-6	GAGGATACCACTCCCAACAGACC	AAGTGCATCATCGTTGTTCATACA
IL-10	CTGGACAACATACTGCTAACCG	GGGCATCACTTCTACCAGGTAA
IP-10	CAAAGCATCCCGTTTCACT	CCCCTTCTTGGTGAGGAATA
KC	ACACTCCAACACAGCACCAT	TGACAGCGCAGCTCATTG
IL-18	CATGTACAAAGACAGTGAAGTAAGAGG	TTTCAGGTGGATCCATTTCC
TNF-α	CATCTTCTCAAAATTCGAGTGACAA	TGGGAGTAGACAAGGTACAACCC
36B4	AGATGCAGCAGATCCGCAT	GTTCTTGCCCATCAGCACC

Table 3. Primers used and their sequences.

as well as protonation and repair of missing residues using the QuickPrep module implemented in MOE with default settings. Subsequently, the structures were subjected to energy minimization with Amber10:EHT force field until the root mean square (RMS) gradient fell below 0.1 cal.mol^{-1}. This process was undertaken to minimize contacts among hydrogen atoms and to obtain a stabilized conformer of the protein. The ligand binding sites were identified and highlighted using the site finder module, which is implemented in the MOE software and the most hydrophobic residues found were selected by dummy atoms. Ligand Preparation and the 2D-to-3D conversion was performed using LigPrep tool, a module of the Small-Molecule Drug Discovery Suite in Schrödinger software package (version 2024-1, Schrödinger, LLC, New York, NY, USA, 2024), followed by an optimization and calculation of single point energy that were carried out using Jaguar v.12.3 (Schrödinger, LLC, NY, 2024)[53] and employing the B3LYP/6-31G** functional basis sets designed for DFT as a level of theory. Finally, after optimization, the ligand was placed into binding site (dummy atoms) of the receptor using Dock module of the MOE software. Default triangle matcher method was used for ligand placement, as well as the induced fit method was used as a refinement method. The conformations were scored by London dG and GBVI/WSA dG. All these above was carried out with the Amber10:EHT force field. The most optimal conformation for the compound was selected based on the S score, with the unit for the scoring function being Kcal/mol. The S score represents the final score, which is the score of the last stage. In regard to the scoring function, a lower score indicates a more favorable pose.

In silico pharmacokinetic profile and drug-likeness prediction

Drug-likeness analysis of fupenzic acid was performed using the SwissADME (http://www.swissadme.ch/)[55] server based on Lipinski's and Veber's rules[55,56]. The calculated physicochemical parameters included molecular weight (MW), lipophilicity (Log P), solubility, number of rotational bonds (nRB), number of hydrogen bond acceptor (nHBA) and donor groups (nHBD), and topological polar surface area (TPSA). According to Lipinski's rule, effective oral drugs should meet the following criteria: MW ≤ 500 Da; nHBA ≤ 10; nHBD ≤ 5; and logarithm of the octanol-water partition coefficient (Log P) ≤ 5; with at most one violation allowed. Moreover, Veber's rule specifies that TPSA must be ≤ 140 Å and nRB ≤ 10. Additionally, pharmacokinetic parameters such as absorption, distribution, metabolism, excretion and toxicity (ADMET) of fupenzic acid were calculated using pkCSM server (https://biosig.unimelb.edu.au/pkcsm/)[58].

Statistical analysis

The data are expressed as means ± standard deviation (SD) from at least three independent experiments. Statistical significance of the data was determined using one-way ANOVA followed by Dunnett's post-hoc test. The threshold for statistical significance was set at $p < 0.05$. Statistical significance levels are indicated as follows: * $p < 0.05$, ** $p < 0.01$ and *** $p < 0.001$. All statistical analyses and the estimation of the half-maximal inhibitory concentration (IC_{50}) values for the effects of fupenzic acid on cell viability and NO release were performed using GraphPad Prism Software 10 (CA, USA).

Data availability

All data generated or analysed during this study are included in this published article and its supplementary information files.

Received: 28 October 2024; Accepted: 15 April 2025
Published online: 24 April 2025

References

1. Caliskan, O. In *The Mediterranean Diet* (eds Victor R. Preedy & Ronald Ross Watson), 621–628 (Academic Press, 2015).
2. Nazhand, A. et al. Hawthorn (Crataegus spp.): An updated overview on its beneficial properties. **11**, 564 (2020).
3. Venskutonis, P. R. & J. J. O. F. B. Phytochemical composition and bioactivities of Hawthorn (Crataegus spp.): review of recent research advances. **4**, 69–87 (2018).
4. Edwards, J. E., Brown, P. N., Talent, N., Dickinson, T. A. & Shipley, P. R. A review of the chemistry of the genus Crataegus. *Phytochemistry* **79**, 5–26. https://doi.org/10.1016/j.phytochem.2012.04.006 (2012).

5. Rjeibi, I., Zaabi, R. & Jouida, W. Characterization of polysaccharides extracted from pulps and seeds of Crataegus azarolus L. var. aronia: Preliminary structure, antioxidant, antibacterial, α-amylase, and acetylcholinesterase inhibition properties. *Oxidative medicine and cellular longevity* 1903056, (2020). https://doi.org/10.1155/2020/1903056 (2020).
6. Yahyaoui, A. et al. Investigation on the chemical composition and antioxidant capacity of extracts from Crataegus azarolus L.: effect of growing location of an important Tunisian medicinal plant. *Chem. Afr.* **2**, 361–365. https://doi.org/10.1007/s42250-019-00054-1 (2019).
7. Wang, X. et al. Chemical constituents, antioxidant and Gastrointestinal transit accelerating activities of dried fruit of Crataegus dahurica. *Food Chem.* **246**, 41–47. https://doi.org/10.1016/j.foodchem.2017.11.011 (2018).
8. Qi-Jie, Z. et al. Triterpenoids from the fruits of wild species of Crataegus scabrifolia and their lipid-lowering activities. *Russ. J. Bioorg. Chem.* **48**, 1291–1298. https://doi.org/10.1134/S1068162022060292 (2022).
9. ULC, C. C. G. 910–1010Sherbrooke St. W. Montreal, QC H3A 2R7, Canada (2024).
10. Panne, D., Maniatis, T. & Harrison, S. C. An atomic model of the interferon-beta enhanceosome. *Cell* **129**, 1111–1123. https://doi.org/10.1016/j.cell.2007.05.019 (2007).
11. The PyMOL. Molecular Graphics System v. v2.5.8.
12. Fang, J., Liu, C., Wang, Q., Lin, P. & Cheng, F. In Silico polypharmacology of natural products. *Brief. Bioinform.* **19**, 1153–1171. https://doi.org/10.1093/bib/bbx045 (2018).
13. Weiss, U. & Inflammation *Nature* **454**, 427, doi:https://doi.org/10.1038/454427a (2008).
14. Gordon, S. & Martinez, F. O. Alternative activation of macrophages: mechanism and functions. *Immunity* **32**, 593–604. https://doi.org/10.1016/j.immuni.2010.05.007 (2010).
15. Liu, G. & Yang, H. Modulation of macrophage activation and programming in immunity. *J. Cell. Physiol.* **228**, 502–512. https://doi.org/10.1002/jcp.24157 (2013).
16. Deng, W., Du, H., Liu, D., Ma, Z. & Editorial The role of natural products in chronic inflammation. **13**. https://doi.org/10.3389/fphar.2022.901538 (2022).
17. Kadasah, S. F. & Radwan, M. O. Overview of ursolic acid potential for the treatment of metabolic disorders, autoimmune diseases, and cancers via nuclear receptor pathways. *Biomedicines* **11** https://doi.org/10.3390/biomedicines11102845 (2023).
18. Mioc, M. et al. Recent advances regarding the molecular mechanisms of triterpenic acids: A review (part II). *Int. J. Mol. Sci.* **23**. https://doi.org/10.3390/ijms23168896 (2022).
19. Banno, N. et al. Triterpene acids from the leaves of Perilla frutescens and their anti-inflammatory and antitumor-promoting effects. *Biosci. Biotechnol. Biochem.* **68**, 85–90. https://doi.org/10.1271/bbb.68.85 (2004).
20. Kawai, T. & Akira, S. Signaling to NF-kappaB by toll-like receptors. *Trends Mol. Med.* **13**, 460–469. https://doi.org/10.1016/j.molmed.2007.09.002 (2007).
21. Fukumitsu, S., Villareal, M. O., Fujitsuka, T., Aida, K. & Isoda, H. Anti-inflammatory and anti-arthritic effects of pentacyclic triterpenoids maslinic acid through NF-kappaB inactivation. *Mol. Nutr. Food Res.* **60**, 399–409. https://doi.org/10.1002/mnfr.201500465 (2016).
22. de las Heras, B. & Hortelano, S. Molecular basis of the anti-inflammatory effects of terpenoids. *Inflamm. Allergy Drug Targets*. **8**, 28–39. https://doi.org/10.2174/187152809787582534 (2009).
23. Nguyen, H. N. et al. Ursolic acid and related analogues: triterpenoids with broad health benefits. *Antioxidants (Basel Switzerland)* **10**. https://doi.org/10.3390/antiox10081161 (2021).
24. Jain, H., Dhingra, N., Narsinghani, T. & Sharma, R. Insights into the mechanism of natural terpenoids as NF-kappaB inhibitors: an overview on their anticancer potential. *Exp. Oncol.* **38**, 158–168 (2016).
25. Li, C. et al. Maslinic acid potentiates the anti-tumor activity of tumor necrosis factor alpha by inhibiting NF-kappaB signaling pathway. *Mol. Cancer*. **9**, 73. https://doi.org/10.1186/1476-4598-9-73 (2010).
26. Salminen, A., Lehtonen, M., Suuronen, T., Kaarniranta, K. & Huuskonen, J. Terpenoids: natural inhibitors of NF-κB signaling with anti-inflammatory and anticancer potential. *Cell. Mol. Life Sci.* **65**, 2979–2999. https://doi.org/10.1007/s00018-008-8103-5 (2008).
27. Sun, L. D. et al. Development and mechanism investigation of a new Piperlongumine derivative as a potent anti-inflammatory agent. *Biochem. Pharmacol.* **95**, 156–169. https://doi.org/10.1016/j.bcp.2015.03.014 (2015).
28. Li, W. et al. Oleanolic acid improves obesity-related inflammation and insulin resistance by regulating macrophages activation. *Front. Pharmacol.* **12**, 697483. https://doi.org/10.3389/fphar.2021.697483 (2021).
29. Mallavadhani, U. V., Panda, A. K. & Rao, Y. R. Diospyros melanoxylon leaves: a rich source of pentacyclic triterpenes. *Pharm. Biol.* **39**, 20–24. https://doi.org/10.1076/phbi.39.1.20.5941 (2001).
30. Castola, V., Bighelli, A. & Casanova, J. Direct qualitative and quantitative analysis of triterpenes using 13 C NMR spectroscopy exemplified by dichloromethanic extracts of Cork. *Appl. Spectrosc.* **53**, 344–350. https://doi.org/10.1366/0003702991946569 (1999).
31. Siddiqui, S., Siddiqui, B. S. & Adil, Q. Begum. Constituents of Mirabilis jalapa. *Fitoterapia* **65**, 471 (1990).
32. Seebacher, W., Simic, N., Weis, R., Saf, R. & Kunert, O. Complete assignments of 1H and 13 C NMR resonances of oleanolic acid, 18α-oleanolic acid, ursolic acid and their 11-oxo derivatives. *Magn. Reson. Chem.* **41**, 636–638. https://doi.org/10.1002/mrc.1214 (2003).
33. Li, Q. J. et al. Chemical constituents from medical and edible plants of Rosa roxburghii. *Zhongguo Zhong Yao Za Zhi*. **41**, 451–455. https://doi.org/10.4268/cjcmm20160316 (2016).
34. Xu, H. X., Zeng, F. Q., Wan, M. & Sim, K. Y. Anti-HIV triterpene acids from Geum Japonicum. *J. Nat. Prod.* **59**, 643–645. https://doi.org/10.1021/np960165e (1996).
35. Brieskorn, C. H. Chemical composition of Apple peels. IV. Pomolic and pomonic acids. *Chem. Ber.* **100**, 1252–1265 (1967).
36. Rongshen Wang, J. S. et al. Chemical constituents isolated from the roots of Sanguisorba officinalis L. and their chemotaxonomic significance. *Biochem. Syst. Ecol.* **89**. https://doi.org/10.1016/j.bse.2019.103999 (2020).
37. Guise, G. B., Ritchie, E. & Taylor, W. C. Further constituents of alphitonia species. *Aust. J. Chem.* **15**, 314–321. https://doi.org/10.1071/CH9620314 (1962).
38. Huo, Y. et al. Isolation and simultaneous quanti Fi cation of nine triterpenoids from Rosa davurica pall. *J. Chromatogr. Sci.* **55**, 130–136. https://doi.org/10.1093/chromsci/bmw155 (2017).
39. Park, K. J., Subedi, L., Kim, S. Y., Choi, S. U. & Lee, K. R. Bioactive triterpenoids from twigs of Betula Schmidtii. *Bioorg. Chem.* **77**, 527–533. https://doi.org/10.1016/j.bioorg.2018.02.006 (2018).
40. Mahmud, S. A., Al-Habib, O. A. M., Bugonl, S., Clericuzio, M. & Vidari, G. A new Ursane-type triterpenoid and other constituents from the leaves of Crataegus azarolus Var. aronia. *Nat. Prod. Commun.* **11**, 1637–1639 (2016).
41. Montilla, M. P. et al. Antioxidant activity of maslinic acid, a triterpene derivative obtained from Olea europaea. *Planta Med.* **69**, 472–474. https://doi.org/10.1055/s-2003-39698 (2003).
42. Eldeen, I. M., Van Heerden, F. R. & Van Staden, J. Isolation and biological activities of termilignan B and Arjunic acid from Terminalia sericea roots. *Planta Med.* **74**, 411–413. https://doi.org/10.1055/s-2008-1034357 (2008).
43. Daina, A., Michielin, O. & Zoete, V. SwissTargetPrediction: updated data and new features for efficient prediction of protein targets of small molecules. *Nucleic Acids Res.* **47**, W357-W364. https://doi.org/10.1093/nar/gkz382 (2019).
44. Nickel, J. et al. SuperPred: update on drug classification and target prediction. *Nucleic Acids Res.* 42, W26-W31. https://doi.org/10.1093/nar/gku477 (2014).
45. Yao, Z. J. et al. TargetNet: a web service for predicting potential drug–target interaction profiling via multi-target SAR models. *J. Comput. Aided Mol. Des.* **30**, 413–424. https://doi.org/10.1007/s10822-016-9915-2 (2016).

46. Huang da, W., Sherman, B. T. & Lempicki, R. A. Systematic and integrative analysis of large gene lists using DAVID bioinformatics resources. *Nat. Protoc.* **4**, 44–57. https://doi.org/10.1038/nprot.2008.211 (2009).
47. Huang da, W., Sherman, B. T. & Lempicki, R. A. Bioinformatics enrichment tools: paths toward the comprehensive functional analysis of large gene lists. *Nucleic Acids Res.* **37**, 1–13. https://doi.org/10.1093/nar/gkn923 (2009).
48. Han, H. et al. TRRUST v2: an expanded reference database of human and mouse transcriptional regulatory interactions. *Nucleic Acids Res.* **46**, D380–D386. https://doi.org/10.1093/nar/gkx1013 (2018).
49. Szklarczyk, D. et al. The STRING database in 2023: protein-protein association networks and functional enrichment analyses for any sequenced genome of interest. *Nucleic Acids Res.* **51**, D638–D646. https://doi.org/10.1093/nar/gkac1000 (2023).
50. Chin, C. H. et al. CytoHubba: identifying hub objects and sub-networks from complex interactome. *BMC Syst. Biol.* **8**. https://doi.org/10.1186/1752-0509-8-S4-S11 (2014).
51. Heberle, H., Meirelles, G. V., da Silva, F. R., Telles, G. P. & Minghim, R. InteractiVenn: a web-based tool for the analysis of sets through Venn diagrams. *BMC Bioinform.* **16**. https://doi.org/10.1186/s12859-015-0611-3 (2015).
52. Zeini, M. et al. Specific contribution of p19(ARF) to nitric oxide-dependent apoptosis. *J. Immunol.* **177**, 3327–3336. https://doi.org/10.4049/jimmunol.177.5.3327 (2006).
53. Cuadrado, I. et al. Labdanolic acid Methyl ester (LAME) exerts anti-inflammatory effects through Inhibition of TAK-1 activation. *Toxicol. Appl. Pharmcol.* **258**, 109–117. https://doi.org/10.1016/j.taap.2011.10.013 (2012).
54. Schrödinger *Release 2024-1: Jaguar V. V.12.3* (2024).
55. Daina, A., Michielin, O. & Zoete, V. SwissADME: a free web tool to evaluate pharmacokinetics, drug-likeness and medicinal chemistry friendliness of small molecules. *Sci. Rep.* **7**, 42717. https://doi.org/10.1038/srep42717 (2017).
56. Lipinski, C. A. Lead- and drug-like compounds: the rule-of-five revolution. *Drug Discovery Today Technol.* **1**, 337–341. https://doi.org/10.1016/j.ddtec.2004.11.007 (2004).
57. Veber, D. F. et al. Molecular properties that influence the oral bioavailability of drug candidates. *J. Med. Chem.* **45**, 2615–2623. https://doi.org/10.1021/jm020017n (2002).
58. Pires, D. E., Blundell, T. L., Ascher, D. B. & pkCSM Predicting small-molecule Pharmacokinetic and toxicity properties using graph-based signatures. *J. Med. Chem.* **58**, 4066–4072. https://doi.org/10.1021/acs.jmedchem.5b00104 (2015).

Author contributions

Conceptualization: AE-B, BH, SH; Formal analysis: BH, SH; Data curation: DB, IC; Investigation: DB, IC, BH, SH; Methodology: DB, IC, AA; Resources: NDB, AA; Software: AA; Validation: BH, SH; Funding acquisition: AE-B, SH; Supervision: AE-B, BH, SH; Writing - original draft: IC, AE-B, BH, AA. SH; writing - review & editing: IC, NDB, AE-B, BH, AA, SH. All authors thoroughly reviewed the manuscript. All authors read and approved the final version of this manuscript.

Funding

The study was funded by Instituto de Salud Carlos III (PI17CIII/00012, PI20CIII/00018) and Ministerio de Ciencia e Innovación (MCIN/AEI/https://doi.org/10.13039/501100011033/FEDER, UE (PID2022-136549OB-100).

Declarations

Competing interests

The authors declare no competing interests.

Additional information

Supplementary Information The online version contains supplementary material available at https://doi.org/10.1038/s41598-025-98901-4.

Correspondence and requests for materials should be addressed to B.H., A.A. or S.H.